Tumor-Specific Delivery of Histidine-Rich Glycoprotein Suppresses Tumor Growth and Metastasis by Anti-Angiogenesis and Vessel Normalization.

Article *in* Current Gene Therapy · March 2014

DOI: 10.2174/1566523214666140305223912 · Source: PubMed

7 authors, including:

Xiawei Cheng
East China University of Science and Technology
15 PUBLICATIONS **184** CITATIONS
SEE PROFILE

Wei Cheng
Huazhong University of Science and Technology
239 PUBLICATIONS **3,928** CITATIONS
SEE PROFILE

Jianxiang Chen
National Cancer Centre Singapore
38 PUBLICATIONS **833** CITATIONS
SEE PROFILE

Zi-Chun Hua
Nanjing University
157 PUBLICATIONS **2,154** CITATIONS
SEE PROFILE

Send Orders for Reprints to reprints@benthamscience.net

Current Gene Therapy, **2014,** *14,* **75-85**

Tumor-Specific Delivery of Histidine-Rich Glycoprotein Suppresses Tumor Growth and Metastasis by Anti-angiogenesis and Vessel Normalization

Xiawei Cheng[a], Xiaoxin Zhang[a], Wei Cheng[a], Jianxiang Chen[a], Cailie Ma[a], Bingya Yang[a] and Zi-Chun Hua[a,b,*]

[a]*The State Key Laboratory of Pharmaceutical Biotechnology, School of Life Science and School of Stomatology, Affiliated Stomatological Hospital, Nanjing University, Nanjing, 210093, Jiangsu, China;* [b]*Changzhou High-Tech Research Institute of Nanjing University and Jiangsu TargetPharma Laboratories Inc., Changzhou, 213164, Jiangsu, China*

Abstract: Histidine-proline-rich glycoprotein (HPRG) is a plasma protein of vertebrates, which has potent anti-angiogenic and tumor vessel normalization properties. Attenuated *Salmonella Typhimurium* strain VNP20009 preferentially accumulates and replicates in hypoxic tumor regions. In this study, we engineered VNP20009 to express HPRG under the control of a hypoxia-induced NirB promoter and evaluated the efficacy of the VNP20009-mediated targeted expressionof HPRG (VNP-pNHPRG) on tumor growth in primary and metastatic tumor models. When VNP-pNHPRG was administered to melanoma tumor mice by intraperitoneal injection, the NirB promoter controlled HPRG expression in tumor, which inhibited tumor vessel density and areas as well as regulated vascular normalization. VNP-pNHPRG significantly delayed tumor growth and enhanced survival time in primary B16F10 mice model and markedly suppressed lung metastatic tumor growth and prolonged survival time in B16F10 metastatic tumor models. Furthermore, VNP-pNHPRG down-regulated the HIF-1α-VEGF/Ang-2 signal pathway by altering the hypoxic tumor microenvironment. These results showed that VNP20009-mediated targeted expression of HPRG provides a novel cancer gene therapeutic approach for the treatment of primary and metastatic cancer.

Keywords: VNP20009, histidine-proline-rich glycoprotein, anti-angiogenesis, vessel normalization, tumor growth, tumor metastasis.

INTRODUCTION

Tumor angiogenesis is a pivotal component of cancer growth, including invasion and metastasis [1]. Thus, anti-angiogenic therapy is an attractive strategy for cancer treatment. Several anti-angiogenic therapies are being subjected to clinical trials to test their potential to treat different types of tumors [2, 3]. Anti-angiogenic therapies can inhibit new blood vessel growth into the tumor, which enables tumor expansion. Formed tumor vessels exhibit multiple abnormalities and unconventional morphological features, including loss of arteriole capillary-venule hierarchy, tortuosity, variable diameter, and leakiness [4, 5]. Even perivascular cells, such aspericytes and vascular smooth muscle cells, around tumor vessels show abnormal structural characteristics [6, 7]. These abnormal tumor vessels not only alter the tumor microenvironment and promote tumor metastasis, but also pose a formidable challenge to antitumor drugs [8]. Thus, suppressing tumor vessels and promoting tumor normalization are important to inhibit tumor growth and metastases.

Histidine-proline-rich glycoprotein (HPRG) is a plasma protein of vertebrates belonging to the cystatin superfamily [9, 10]. HPRG can interact with numerous ligands (C1q, IgG, and FcR) and has multiple important biological functions, including immune responses by modulating the formation of immune complexes and necrotic cell clearance, as well as potent anti-angiogenic and tumor vessel normalization properties [11-15]. These properties highlight the potential of HRPG for using as an anti-cancer and anti-angiogenic agent in the future. However, systemic administration of HRPG may have weak tumor targeting and low bioavailability. Thus, the ideal application of HPRG in cancer therapy needs its targeted delivery to hypoxic tumor regions and abnormal vessels and tissue-specific execution of its antitumor activity.

Facultative anaerobe *Salmonella Typhimurium* strains provide a potential solution to mediate anti-angiogenic drugs and other anticancer agents to target hypoxic tumor regions for preferential accumulation and replication in hypoxic regions of solid tumors [16, 17]. To diminish the potential toxicity to induce tumor necrosis factor-α and cause septic shock, attenuated *S. typhimurium* VNP20009 was developed by a genetically modified method that deletes purI and msbB genes [18, 19]. More studies showed that VNP20009 alone [20, 21] or mediated anticancer agents such as endostatin [22], TRAIL [23] and CCL21 [24] can suppress tumor growth and prolong survival time in murine tumor models. VNP20009 has not exhibited antitumor activity on phase I human clinical trials, but has an acceptable safety profile

*Address correspondence to this author at the Department of Biochemistry, Nanjing University, 22 Hankou Road, Nanjing, Jiangsu Province, P.R. China; Tel: +86-25-8332-4605; Fax: +86-25-8332-4605;
E-mail: zchua@nju.edu.cn

1875-5631/14 $58.00+.00

[25]. Given its safety and tumor-targeting specificity, we select VNP20009 as a drug delivery system to mediate HPRG to target tumor tissues. What is more interesting is that VNP20009 can inhibit tumor blood vessel growth by down-regulating vascular endothelial growth factor (VEGF) protein levels in tumor tissues [26]. Therefore, we hypothesized that VNP20009-mediated tumor-targeted HPRG gene has the potential to enhance the antitumor effect by inhibiting tumor angiogenesis and promoting tumor vessel normalization properties.

In this study, we engineered VNP20009 to express HPRG under the control of a hypoxia-induced NirB promoter in tumor tissues. We evaluated the efficacy and mechanism of the VNP20009-mediated targeted expression of HPRG (VNP-pNHPRG) on tumor growth in primary and metastatic tumor models. We found that VNP-pNHPRG can preferentially accumulate and effectively control HRPG expression in tumor tissues. VNP-pNHPRG can inhibit angiogenesis and regulate vessel normalization *in vivo*. VNP-pNHPRG can significantly suppress tumor growth and metastasis and prolong survival time in murine tumor models.

MATERIALS AND METHODS

Animals, Cell Lines, Gene, Plasmids and Bacterial Strains

Five- to six-week-old male C57BL/6 mice were obtained from the Comparative Medicine Center of Yangzhou University and maintained in pathogen-free conditions for one week before the start of the experiment. B16F10 melanoma cells were purchased from American Type Culture Collection (ATCC, USA). Cell lines were cultured at 37°C in 5% CO_2 in a humidified atmosphere in Dulbecco's modified Eagle's media (DMEM) supplemented with 10% fetal bovine serum (FBS). HPRG gene was obtained from cDNA of mice liver tissue by reverse transcription-polymerase chain reaction (RT-PCR). Lpp-ompA-luciferase gene and plasmid pQE30-NirB were maintained in our laboratory. *S. typhimurium* VNP20009 ($msbB^-/purI^-$) was purchased from ATCC (USA) and cultured in modified Luria-Bertani (LB) media at 37°C. *S. typhimurium* VNP20009 ($msbB^-/purI^-$) was abbreviated to VNP.

Plasmid Construction and Bacterial Transformation

Two pairs of primers, including *KpnI* and *HindIII* (the restriction enzyme encoding sequences were italic), were designed to amplify HPRG and Lpp-ompA-luciferase gene. Primers sequences follow as:

H1: 5'- CGC*GGATCC*ATGGTGGACCACAGTCAAGGATG-3';

H2: 5'- CCC*AAGCTT*TTATTTTGGAGGTGTATATCCAAAAAAC-3';

L1: 5'-CGC*GGATCC*ATGAAAGCTACTAAACTG-3';

L2: 5'-CCC*AAGCTT* TTACACGGCGATCTTTCC-3'.

HPRG and Lpp-ompA-luciferase gene were ligated into pQE30-NirB vector by PCR amplification. HPRG and Lpp-ompA-luciferase proteins were expressed under the control of NirB promoter. The accuracy of HPRG and Lpp-ompA-luciferase gene was confirmed by sequencing. pQE30-NirB, pQE30-NirB-HPRG, and pQE30-NirB-Lpp-ompA-luciferase plasmids were transformed into VNP by a Bio-Rad Micropulserat 2.5 kV, 25 mF and 400 Ω, respectively. Positive VNPs were called VNP-pN, VNP-pNHPRG and VNP-pNLOL.

Construction of Tumor Model

B16F10 melanoma cells, which had been grown in DMEM plus 10% FBS, were collected and suspended in PBS (pH 7.4). We dispersed 2×10^5 cells in 100 μl of PBS, which was then injected subcutaneously into the hind flank region of the C57BL/6 mice.The tumors were allowed to grow. Animal studies designed to maintain a high standard of animal welfare were approved by the Nanjing University Animal Care and Use Committee.

NirB Promoter Function Assay *In vitro* and *In vivo*

VNP-pNHPRG (2×10^9 cfu) was grown at 37°C to the logarithmic phase and was inoculated into 100 ml of LB media and cultured under aerobic and anaerobic conditions. After 3 days, VNP-pNHPRG was harvested by centrifugation at 4°C and suspended in 2 ml of PBS buffer. After repeated sonication, the solution was centrifuged at 4°C, and the supernatant was collected. HPRG expression was analyzed by Western blot. Goat anti-HRPG polyclonal antibody (Santa Cruz, sc-47044) was used to detect HRPG expression.

When the tumor volume reached approximately 150 mm^3 (about 6d to 8d), 2×10^4 cfu VNP-pNLOL/*per* mouse (B16F10) was inoculated by intraperitoneal injection. Luciferase protein expression in tumor was analyzed by optical bioluminescence imaging at 2d and 4d after injection. Bioluminescence imaging was performed using IVIS 100 (Caliper) according to the instructions of the manufacturer.

Analysis of Bacterial Biodistribution

To determine bacterial biodistribution, the B16F10 tumor mice with tumor volume of approximately 150 mm^3 were inoculated with VNP-pNHPRG by intraperitoneal injection. Mice were sacrificed after 3 d and 6 d. The tissue samples (heart, liver, spleen, lung, kidney and tumor) were weighed and homogenized in a known volume of PBS and plated on LB agar containing 50 μg/ml ampicillin by serial dilution. After 16 h of culture at 37°C, colony numbers were counted.

Anti-tumor Analysis of VNP-pNHPRG *In vivo*

B16F10 tumor mice with tumor volume of 100 mm^3 to 150 mm^3 were randomly divided, with 2×10^4 cfu VNP, VNP-pN and VNP-pNHPRG *per* mouse, respectively. The length and width of the tumor were measured every two days using a Vernier caliper (Mytutoyo Corporation, Japan) across its two perpendicular diameters. Tumor volume was calculated using the following formula: tumor volume = $length\times width^2\times0.52$. The numbers and dates of death of mice were recorded to calculate the survival rate.

VNP-pNHPRG Therapy of Tumor Metastasis

Forty female C57BL/6 mice were used to obtain metastasis models. B16F10 cells (2×10^5 in 200 μl of PBS) were inoculated in the tail vein of C57BL/6 mice. Mice were ran-

domly divided into four groups: PBS, VNP, VNP-pN and VNP-pNHPRG groups. After 3 and 12 days, the mice in the PBS group were injected intraperitoneally with 100 μl of PBS *per* mouse, whereas the mice in the VNP, VNP-pN and VNP-pNHPRG groups were injected intraperitoneally with 2×10^4 cfu VNP, VNP-pN and VNP-pNHPRG *per* mouse, respectively. After 20 days, mice were sacrificed and the numbers of lung metastasis were counted. The numbers and dates of death of mice were recorded to calculate the survival rate.

Endothelial Cell Proliferation Assay *In vitro*

Endothelial cell proliferation was analyzed by the xCELLigence system. The xCELLigence system can detects real-time proliferation, invasion and migration of cells without the use of labels. The method is widely used to analyze cell proliferation and migration [27, 28]. In brief, HUVECs cells (passage 2) were grown and expanded in DMEM (15% FBS,100 μg/ml ECGS, 10 μg/ml heparin sodium). After reaching ~75% confluence, HUVECs cells were washed with PBS, afterwards detached from the flasks with trypsin/EDTA. Subsequently, 100 μL of DMEM (2% FBS, 100 μg/ml ECGS, 10 μg/ml heparin sodium , 10 μM $ZnCl_2$) at room temperature was added into each well of E-plate 16. After this the E-plate 16 was connected to the system and checked in the cell culture incubator for proper electrical-contacts and the background impedance was measured during 40 s. Meanwhile, HUVECs cells were resuspended in DMEM (2% FBS, 100 μg/ml ECGS, 10 μg/ml heparin sodium, 10 μM $ZnCl_2$) and adjusted to 1×10^5 cells/ml was added to the 100 μL medium containing wells on E-plate 16. HUVECs cells were treated with VNP-pN lysate supernatant (total at protein 200 μg/ml) and VNP-pNHPRG (50 and 200 μg/ml). Controls received with PBS only. After 30 mins incubation at room temperature, E-plate 16 was placed into the cell culture incubator. Finally, proliferation of the cells was monitored every 1 h for a period of up to 40 h via the incorporated sensor electrode arrays of the E-Plate 16. The electrical impedance was measured by the RTCA-integrated software of the xCELLigence system (Roche) as a dimensionless parameter termed CI. Triplicate experiments were performed in a parallel manner for each concentration point.

Immunohistochemistry, Hematoxylin and Eosin (H&E) Staining and Immunofluorescence Microscopy

After treatment for 6 days, mice in PBS, VNP, VNP-pN and VNP-pNHPRG groups were sacrificed. Frozen tumor sections were prepared using the afore mentioned procedure and incubated with rabbit polyclonal antibody against *Salmonella* (Abcam, ab69254) and goat anti-HRPG polyclone antibodies (Santa Cruz, sc-47044) to analyze VNP location and HPRG expression in tumor. H&E staining was performed to analyze lung tumor infiltration according to standard protocols. Immunofluorescence was conducted to explore vascular density/areas and vascular normalization. The tumor vascularity was stained with rat anti-mouse CD31 (BD Pharmingen™, USA). The secondary antibodies for CD31 were goat anti-rat IgG labeled with Cy3 (Jackson ImmunoResearch, USA). Vessel density was determined by averaging the number of vessels. Vessel areas were determined by averaging the areas of vessels in six areas with the highest vessel density at ×200 magnification in each section. Tumor vascular pericytes were examined with rabbit anti-desmin polyclonal antibody (Santa Cruz, sc-14026). The secondary antibodies for CD31 were goat anti-rat IgG labeled with Cy3. The secondary antibodies for desmin were goat anti-mouse IgG labeled with FITC (Invitrogen, USA). Hypoxia-inducible factor-1α (HIF-1α) expression in tumor tissues was analyzed by immunofluorescence. HIF-1α protein was stained with rabbit anti-mouse HIF-1α (Santa Cruz, sc-14026). The secondary antibodies were goat anti-rabbit IgG labeled with FITC (Invitrogen, USA).

Real-time Quantitative PCR Assay

Total RNA was isolated from tumor tissues with TRIzol reagent (Invitrogen). cDNA was synthesized using ReverTra Ace® qPCR RT Kit (Toyobo). Real-time quantitative PCR was performed to determine VEGF and Ang-2 expression.To analysis HIF-1α, VEGF and Ang-2 expression, primers were synthesized as follows:

β-actin sense, 5'-ATATCGCTGCGCTGGTCGTC-3',

β-actin antisense, 5'-AGGATGGCGTGAGGGAGAGC-3';

HIF-1α sense, 5'- GCTCCCTATATCCCAATGGAT-3',

HIF-1α antisence, 5'- CCATCATGTTCCATTTTTCGC -3';

VEGF sense, 5'-GGAGATCCTTCGAGGAGCACTT-3',

VEGF antisence, 5'-GGCGATTTAGCAGCAGATATAA-GAA-3';

Ang-2 sense, 5'-GCATGACCTAATGGAGACCGTC-3';

Ang-2 antisence, 5'-GATAGCAACCGAGCTCTTGGAG-3'.

Quantitative RT-PCR was performed with FastStart Universal SYBR Green PCR Master (Roche, USA) and StepOne Real-Time PCR System (Applied Biosystems, USA). The data were analyzed by StepOne Software 2.1 (Applied Biosystems, USA) according to the manufacturer's specifications. The relative mRNA expression levels of HIF-1α, VEGF and Ang-2 in each tumor tissue were calculated from the corresponding standard curve by the indicated software and normalized with the β-actin level in the same sample.

Scanning Electrochemical Microscope (SEM)

Tumor tissues (5 mm ×5 mm) were first treated with PBS, VNP, VNP-pN and VNP-pNHPRG, fixed by 3% glutaraldehyde above 2 h, and then dehydrated using serial dilutionsof hexanenitrile (50%, 70%, 80%, 90% and 100%). Samples were dried by lyophilization. Vascular morphology was observed by SEM (S-3400N II, Hitachi Corporation, Japan).

Two-Photon Microscopy

After treatment for 6 days, mice in PBS, VNP-pN and VNP-pNHPRG groups were anesthetized using 100 μl 1% pentobarbital sodium dissolved in 100 ml PBS by intraperitoneal injection. Check for lack of toe pinch reflex to ensure an adequate level of anesthesia. 100 μl 10 mg/ml FITC-dextran (Sigma-Aldrich, USA) was injected *via* tail vein to visualize the blood stream. After injection 15 min, mice were sacrificed and tumor tissues were obtained. Vascular morphology was observed by two-photon microscopy (Leica, Germany).

Statistical Analysis

The results are presented as mean ± SD. Data were analyzed using the SPSS 13.0 software. Analysis of variance followed by the least significant difference test was used for multiple comparisons. The effect of treatment on survival time was determined using the log-rank test. The level of significance was set at $P < 0.05$.

RESULTS

VNP-pNHPRG Preferentially Accumulate in Tumor Tissue

To determine the bacterial biodistribution, VNP-pNHPRG was inoculated into B16F10 tumor mice. At 3 days post-injection, the tissues were removed and homogenized, VNP-pNHPRG was isolated. After 3 days, VNP-pNHPRG preferentially accumulated in tumors (Fig. **1A** and **1B**). The number of VNP-pNHPRG reached 8.0×10^8 cfu/g (Fig. **1E**). Apart from tumor tissues, VNP-pNHPRG also localized to normal tissues such as the spleen (5.0×10^5 cfu/g) and liver (1.0×10^5 cfu/g) (Fig. **1C**-**1E**). VNP-pNHPRG was not detected in the heart, lung, and kidney (the data not shown). After 6 days, VNP-pNHPRG in tumors still accumulated (8.0×10^8 cfu/g), but VNP-pNHPRG in both the spleen and liver dropped to less than 1000 cfu/g (Fig. **1E**). These results demonstrate that the intraperitoneal injection of VNP-pNHPRG can preferentially accumulate and remain in large amounts in the tumors. The fact that absence in the most normal tissues and only a small amount, about 1:10000 relative to tumor tissue, of VNP-pNHPRG was retained in spleen and liver tissues, exhibiting its good safety.

HRPG Expressed by VNP Gene Delivery in Tumor Hypoxia Regions Under the Control of NirB Promoter

To analyze the capability of NirB promoter to express exogenous proteins in hypoxic tumor regions, VNP-pNLOL carrying luciferase gene was injected into B16F10 tumor mice. Luciferase protein was observed by IVIS 100 4 days after injection (Fig. **2A** and **2B**). VNP-pNHPRG was cultured under aerobic and anaerobic conditions *in vitro*. Western blot showed that HPRG protein was expressed in anaerobic conditions. However, this expression was not observed under aerobic conditions (Fig. **2C**). Immunohistochemistry assay showed that HPRG protein was expressed in tumor tissues treated by VNP-pNHPRG, but was not detected in the PBS, VNP and VNP-pN groups (Fig. **2D**). Thus, the NirB promoter can control HPRG gene expression in hypoxic tumor regions.

VNP-pNHPRG Inhibited Tumor Angiogenesis and Regulated Vascular Normalization

HPRG has potent anti-angiogenic effects. Thus, we evaluated whether VNP-pNHPRG has anti-angiogenic effects *in vitro* and *in vivo*. The study of *in vitro* results showed that VNP-pNHPRG lysate supernatant significantly inhibited ECGS-stimulated HUVEC cell proliferation in a dose-dependent manner compared with controls or VNP-pN alone, indicating the antiangiogenesis capability of VNP-

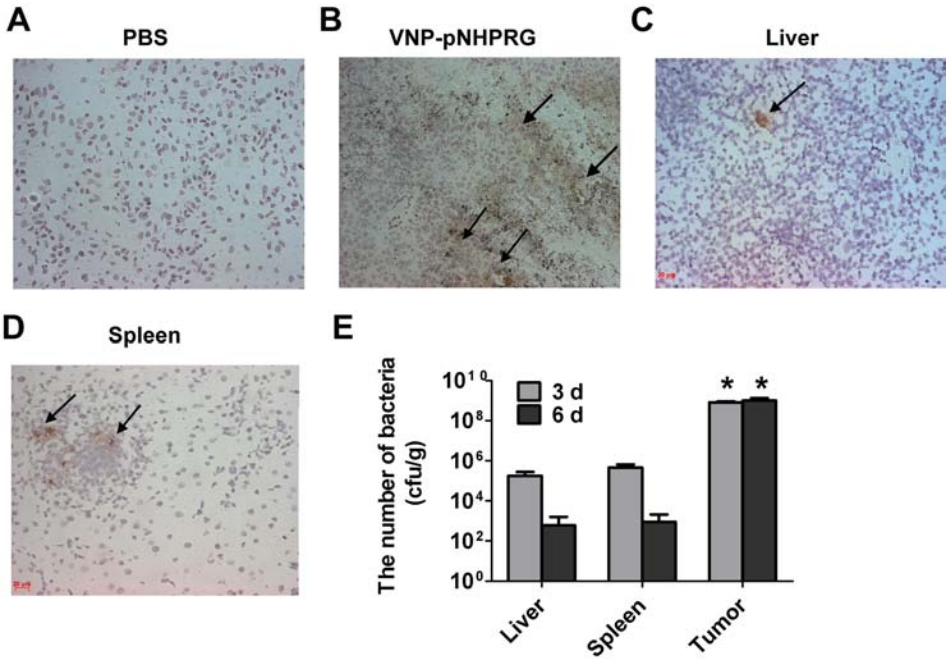

Fig. (1). VNP preferentially accumulate in B16F10 tumor tissue.

(**A-B**) Immunohistochemistry for VNP-pNHPRG (stained brown with blank arrows), revealing VNP-pNHPRG distribution in B16F10 tumor tissue treated with PBS (A) and VNP-pNHPRG (B). (**C-D**) Immunohistochemistry for VNP-pNHPRG (stained brown and indicated with blank arrows), revealing VNP-pNHPRG distribution in liver (C) and spleen (D) in B16F10 tumor model treated with VNP. (**E**) VNP-pNHPRG concentration (cfu/g) in tumor, Liver and Spleen of C57BL/6 bearing B16F10 cells on 3 days and 6 days after intraperitoneal injection of 10000 VNP-pNHPRG *per* mose. Bar represents the mean ± SD of three animals. *$P < 0.001$, tumor compared with Liver and Spleen.

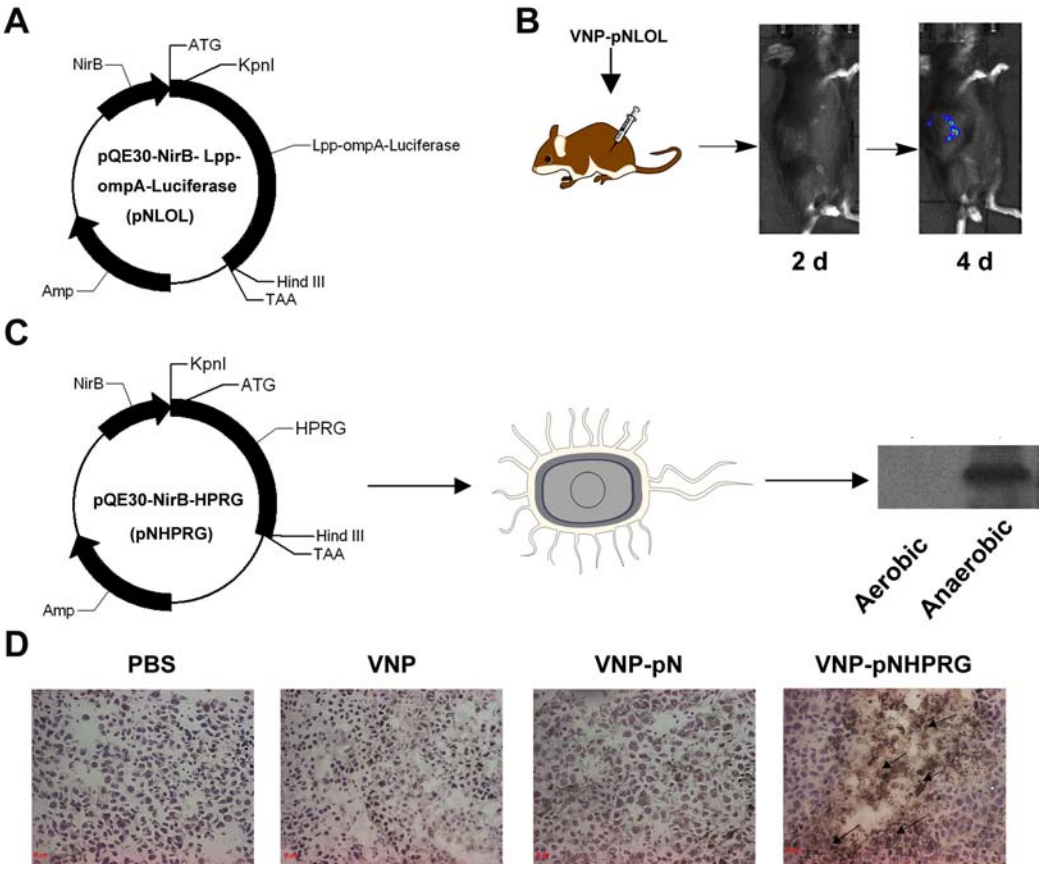

Fig. (2). HRPG expressed by VNP gene delivery in tumor hypoxia regions under the control of NirB promoter.

(**A**) The plasmid constructions of pQE30-NirB- Lpp-ompA-Luciferase (pNLOL) to analyze NirB promoter ability in tumor hypoxia regions. (**B**) Live imaging showed that Luciferase proteins are expressed in B16F10 tumor by VNP gene delivery under the control of NirB promoter on 4 days after intraperitoneal injection of 10000 VNP-pNLOL *per* mose. (**C**) pQE30-NirB-HPRG plasmid (pNHPRG) was constructed and was transformed into VNP (VNP-pNHPRG). VNP-pNHPRG was grown for 24 h under anaerobic or aerobic conditions. Bacterial lysates were subjected to immunoblotting assays using anti-HPRG antibodies. (**D**) Immunohistochemistry for HPRG (stained brown with blank arrows), revealing HPRG distribution in B16F10 tumor tissue treated with PBS, VNP, VNP-pN and VNP-pNHPRG.

pNHPRG (Supplementary Fig. **1A** and **1B**). To evaluate the efficacy of VNP-pNHPRG on tumor vascular density/areas *in vivo*, the endothelial cells of tumor tissue were visualized by CD31 staining. The results show that tumor tissue vascular density/areas in mice inoculated with VNP-pNHPRG significantly decreased compared with that in mice inoculated with PBS, VNP and VNP-pN ($P<0.05$), meanwhile tumor vascular density in mice inoculated with VNP and VNP-pN also decreased than that in mice inoculated with PBS ($P<0.05$) (Fig. **3A-C**). The results of two-photon microscopy also showed that tumor tissue vascular density/areas in mice inoculated with VNP-pNHPRG significantly decreased than that in mice inoculated with PBS and VNP-pN ($P<0.05$). In addition, the branched structure of tumor vessel in mice inoculated with VNP-pNHPRG exhibited two branches, but three or several branches in mice inoculated with PBS and VNP-pN (Fig. **3D**). Double staining for CD31 and desmin in tumor tissue sections facilitated the analysis of tumor vessel normalization. The results show that tumor vessels in VNP-pNHPRG mice were covered by numerous pericytes (Fig. **4A**). By contrast, pericytes of tumor vessels in PBS, VNP and VNP-pN mice were few or rare (Fig. **4A**). The percentage of $desmin^{+}$in $CD31^{+}$ vessels in VNP-pNHPRG mice was significantly enhanced compared with that of PBS, VNP and VNP-pN mice ($P<0.05$)(Fig. **4B**). We analyzed tumor vessel morphology by SEM. Unlike tumor vessels in PBS, VNP and VNP-pN mice, the walls of tumor vessels in VNP-pNHPRG mice showed smooth and regular ultrastructures (Fig. **4C**). The percentage of normalized vessels in VNP-pNHPRG mice was significantly higher than that in PBS, VNP and VNP-pN mice ($P<0.05$) (Fig. **4D**). Thus, VNP-pNHPRG can enhance anti-angiogenic effects of VNP and promote the transformation of tumor vessels from abnormality to normality.

VNP-pNHPRG Delayed Tumor Growth and Enhanced Survival Time in B16F10 Mice Model

To evaluate the antitumor effects of VNP-pNHPRG, VNP, VNP-pN and VNP-pNHPRG were inoculated into B16F10 mice. The tumor volumes of VNP, VNP-pN and VNP-pNHPRG mice were significantly lower than that of PBS mice ($P<0.05$) (Fig. **5A**). The tumor volume in VNP-pNHPRG mice significantly decreased compared with that of VNP and VNP-pN mice ($P<0.05$) (Fig. **5A**). The Kaplan-Meier survival assay showed that the cumulative survival rate and median survival time in VNP-pNHPRG mice sig-

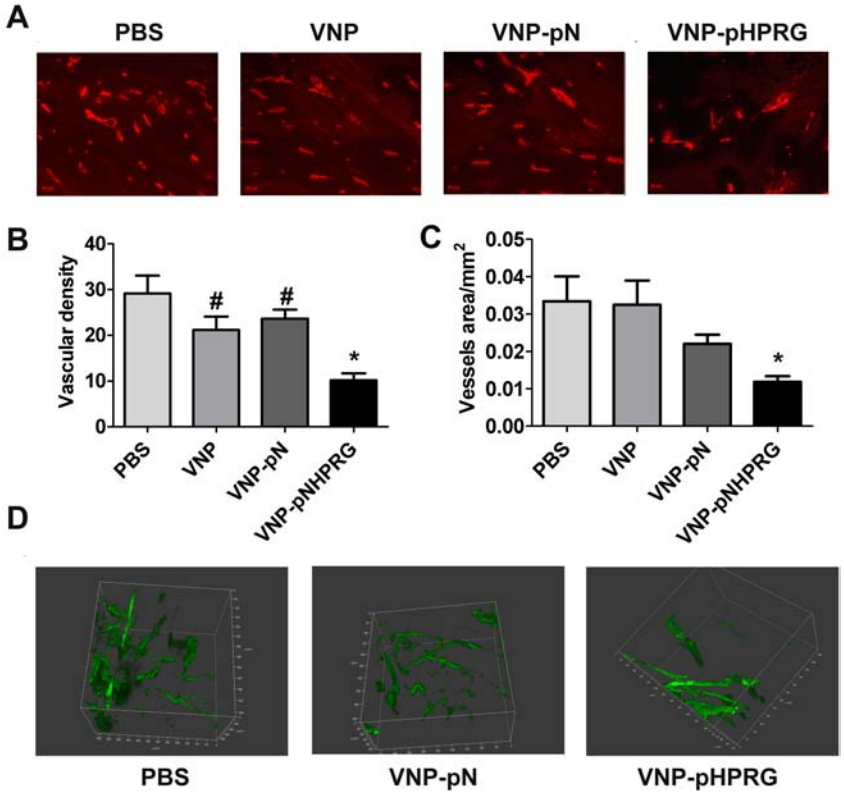

Fig. (3). VNP-pNHPRG inhibited tumor angiogenesis in B16F10 tumor model.

(**A**) Immunofluorescence staining for CD31 (stained red) in tumor tissues of mice treated with PBS, VNP, VNP-pN, and VNP-pNHPRG. (**B**) Quantification of vessels density. Bar represents the mean ± SD of ten tumor tissue sections. *P < 0.05, VNP-pNHPRG compared with PBS, VNP and VNP-pN. #: P<0.05, PBS compared with VNP and VNP-pN. (**C**) Quantification of vessels area. Bar represents the mean ± SD of ten tumor tissue sections. *P < 0.05, VNP-pNHPRG compared with PBS, VNP and VNP-pN. (**D**) Three-dimensional vascular network of two-photon fluorescence microscopy in tumor tissues of mice treated with PBS, VNP-pN and VNP-pNHPRG.

nificantly increased compared with that in PBS, VNP and VNP-pN mice (log-rank tests, P<0.05) (Fig. **5B**). The tumor doubling time was significantly prolonged from 1.32 d (CI, 1.21 d to 1.47 d) in the PBS control group, 2.30 d (CI, 2.10 d to 2.55 d) in VNP group, or 2.36 d (CI, 2.15 d to 2.62 d) in VNP-pN group to 3.80 d (CI, 3.49 d to 4.16 d) in VNP-pNHPRG group (P<0.05) (Fig. **5C** and Supplementary Table **1**). Tumor growth delay also significantly increased from 3.22 d (CI, 2.55 d to 4.06 d) in PBS control group, 6.01 d (CI, 3.68 d to 7.32 d) in VNP group, or 5.55 d (CI, 4.53d to 6.85 d) in VNP-pN group to 9.38 d (CI, 8.24 d to 10.76 d) in VNP-pNHPRG group (P<0.05) (Fig. **5D** and Supplementary Table **1**).

VNP-pNHPRG Delayed Tumor Metastasis in B16F10 Mice Model

To establish a metastasis model, B16F10 cells were injected into the tail vein of C57BL/6 mice. After 2 and 12 days post-injection, PBS, VNP, VNP-pN and VNP-pNHPRG were injected intraperitoneally. Mice were sacrificed, and metastases were counted 30 d after treatment. Although lung metastases were observed on all mice in the four groups (Supplementary Table **2**), the number of lung metastases on the surface of the lung was significantly lower in VNP-pNHPRG mice than that in PBS, VNP and VNP-pN groups, meanwhile VNP and VNP-pN groups also displayed anti-metastatic effect in comparison with PBS control (P <0.05) (Fig. **6A** and **6B**). H&E staining showed B16F10 tumor cell invasion and necrosis in lung tissues of PBS, VNP and VNP-pN mice, but slight tumor cell invasion and inflammation in VNP-pNHPRG mice after 30 d (Fig. **6C**). Intestinal metastasis and axillary lymph node metastasis were also observed in PBS, VNP, VNP-pN and VNP-pNHPRG mice. Compared with the PBS mice, the incidence rate of intestinal metastasis and axillary lymph node metastasis in VNP-pNHPRG mice significantly decreased (P < 0.05) (Supplementary Table **2**). No statistical difference exists among PBS, VNP and VNP-pN mice (P>0.05). The Kaplan-Meier survival assay showed that the cumulative survival rate and median survival time in VNP-pNHPRG mice significantly increased compared with that in PBS, VNP and VNP-pN mice (log-rank tests, P < 0.05) (Fig. **6D**). Thus, VNP-pNHPRG can inhibit tumor metastasis and prolong mice survival time.

VNP-pNHPRG Down-regulated HIF-1*α*, VEGF, and Ang-2 Level in Tumor Tissues

The HIF-1α-VEGF/Ang-2 signal pathway is involved in tumor angiogenesis under hypoxic tumor conditions. Our results showed that the HIF-1α mRNA level in VNP-pNHPRG mice was significantly down-regulated compared with that in PBS, VNP and VNP-pN mice (P<0.05) (Fig. **7A**). Immunofluorescence and its quantitative results also

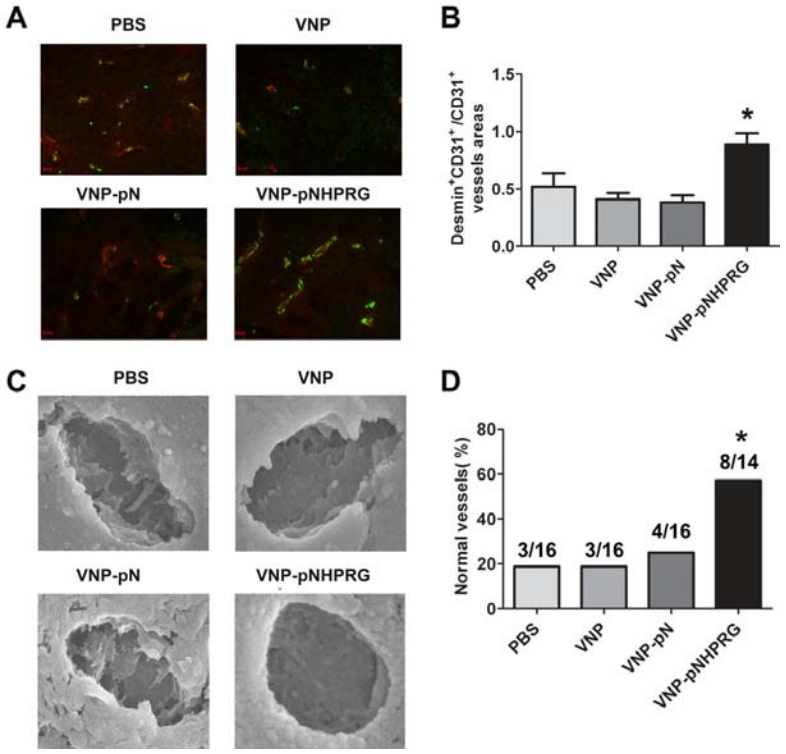

Fig. (4). VNP-pNHPRG regulated vascular normalization in B16F10 tumor model.

(**A**) Immunofluorescence double staining for CD31 (red) and desmin (green) in tumor tissues of mice treated with PBS, VNP, VNP-pN and VNP-pNHPRG, to show tumor vascular Pericytes cells. (**B**) Quantification showed the percentage of desmin$^+$CD31$^+$ vessels areas in CD31$^+$ vessels areas. *P < 0.05. VNP-pNHPRG compared with PBS, VNP and VNP-pN. Bar represents the mean ± SD of six optical fields. (**C**) SEM micrographs showed abnormal tumor vessel including deformed, branched and disconnected ECs with luminal protrusions in tumor tissue of mice treated with PBS, VNP and VNP-pN and normalized vessel in tumor tissue of mice treated with VNP-pNHPRG, which have a relatively uniform size and shape. (**D**) Quantification revealed the percentage of normalized vessel in mice tumor tissues. *P < 0.05, VNP-pNHPRG compared with PBS, VNP and VNP-pN.

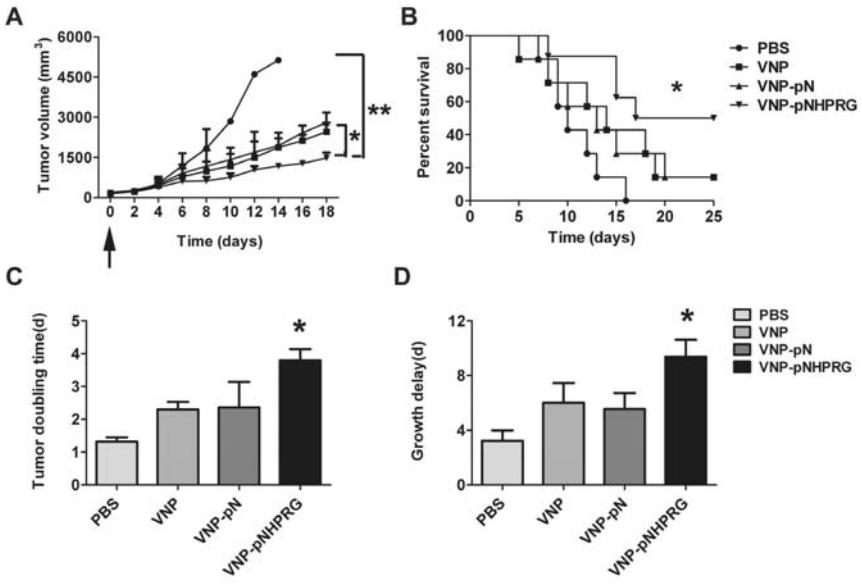

Fig. (5). VNP-pNHPRG delayed tumor growth and enhanced survival time in B16F10 mice model.

(**A**) Tumor growth curves. B16F10 tumor mice per group were injected *i.p.* with 1×10^4 cfu of VNP, VNP-pN, and VNP-pNHPRG, or with PBS at day 7. Tumor volumes among different groups were compared. Data are presented as mean ± SD. *P < 0.05 for VNP-pNHPRG versus VNP and VNP-pN; **P < 0.01 for VNP-pNHPRG versus PBS. (**B**) Kaplan-Meier survival curves of mice bearing B16F10 melanomas. Data were analyzed by the log-rank test. *P < 0.05 for VNP-pNHPRG versus VNP, VNP-pN and PBS. (**C-D**) Tumor doubling time and growth delay. Data are presented as mean ± SD. *P < 0.05 for VNP-pNHPRG versus PBS, VNP and VNP-pN.

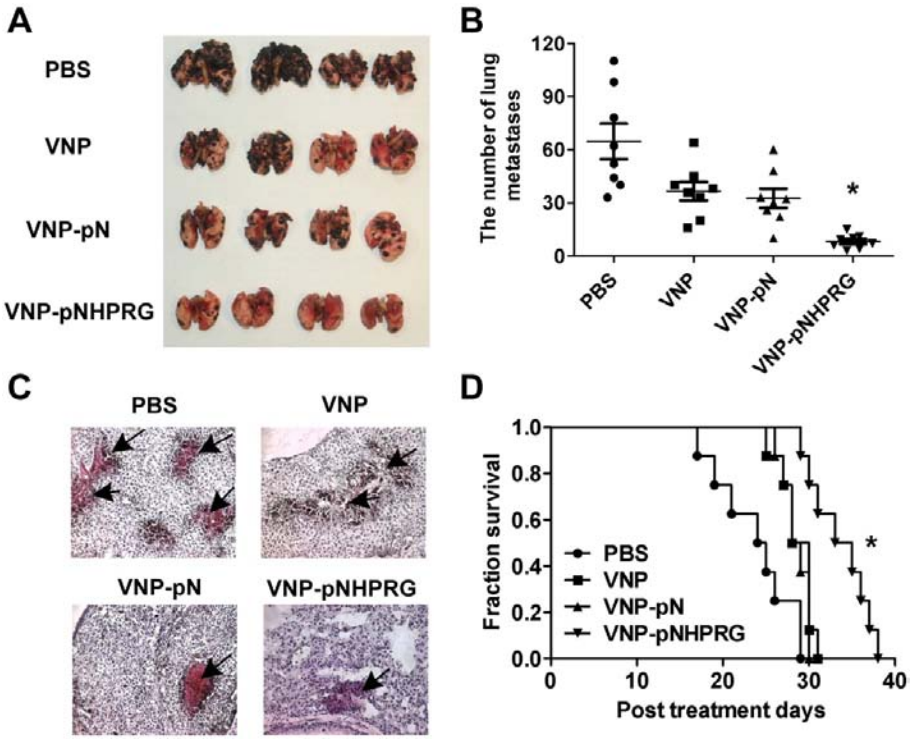

Fig. (6). VNP-pNHPRG retard tumor metastasis in B16F10 mice model.

(**A**) The images of lung metastases. Four lung tissues *per* group were showed. (**B**) The number of metastases on the surface of the lung. Data are presented as mean ± SD. n=8. *P < 0.05 for VNP-pNHPRG versus PBS, VNP and VNP-pN. (**C**) HE staining showed the infiltration of B16F10 melanomas cells in the inside of the lung. (**D**) Kaplan-Meier survival curves of mice on B16F10 metastasis model. Data were analyzed by the log-rank test. *P < 0.05 for VNP-pNHPRG versus PBS, VNP and VNP-pN.

showed that HIF-1α protein level in VNP-pNHPRG mice was significantly down-regulated compared with that in PBS, VNP and VNP-pN mice (P<0.05) (Fig. **7B** and **C**). VEGF and Ang-2 mRNA level in VNP-pNHPRG mice were also significantly down-regulated compared with those in PBS, VNP and VNP-pN mice (P<0.05) (Fig. **7D** and **7E**). VNP and VNP-pN could down-regulate VEGF expression, but did not show any influence on Ang-2 (P<0.05) (Fig. **7D** and **E**), indicating that VNP has the ability of down-regulating VEGF and thus anti-angiogenic function, but inability of regulating tumor vessel normalization. In comparison, VNP-pNHPRG endowed VNP with additional ability of down-regulating the HIF-1α-VEGF/Ang-2 signal pathway, resulting intumor vessel normalization, which can improve tumor oxygenation, thus displaying more potent antitumor efficacy than VNP therapy alone.

CONCLUSION

Angiogenesis is an essential step in tumor proliferation, expansion, and metastasis. Thus, blood vessels in tumors are clinically important therapeutic targets. HPRG is a multi-domain heparin-binding plasma protein. Recent studies showed that HPRG has potent anti-angiogenic properties because of its His/Pro-rich domain, thus offering therapeutic opportunities for anti-cancer and anti-angiogenic treatment [29-32]. However, when HPRG is systemically administered into patients or mice, litter-dose HPRG reaches tumor tissue-sin hypoxic tumor regions and abnormal tumor vessels. To enhance the anti-angiogenic effect, an efficient drug delivery system is needed to target HPRG to the tumor site.

Several facultative anaerobe strains, including *S.typhimurium* [33-35], *Clostridium* [36, 37], *Bifidobacterium* [38] and *E.coli* [39], have significant potential in cancer therapy because of their capability to target the hypoxic region of solid tumors [40]. Attenuated *S.typhimurium* VNP20009 is an outstanding antitumor agent for the inhibition of tumor growth and is a gene delivery vector for the transfer of antitumor agents to tumor sites [41, 26]. Previous reports showed that VNP has been engineered to express numerous proteins, including endostatin, against tumor growth [42, 43]. In our study, VNP carrying a prokaryotic expression vector encoding HRPG under the control of an anaerobic promoter (NirB) was designed to express HPRG protein in tumor tissue and to inhibit tumor angiogenesis. Live imaging and immunohistochemistry showed that VNP-mediated luciferase reporter gene and HPRG gene can express in tumor tissues. The results indicate that the anaerobic-inducible NirB promoter can control HPRG protein expression in hypoxic tumor regions rather than in normal tissues. Aside from the high levels of HPRG expression in the tumor site, lower pH of the tumor microenvironment can enhance the biological activity of HPRG.

HPRG (especially His/Pro-rich domain) acts as a pH sensor [44]. HPRG exposure to low pH promotes the binding of HPRG to endothelial cells because of the protonation of abundant Histidine residues of the H/P domain. The hypoxic regions of solid tumors provide a lower pH microenvironment for predominant glycolytic metabolism (Warburg effect) and poor fluid clearance for tumor vessel abnormalities [45]. When VNP targeting HPRG was expressed in hypoxic

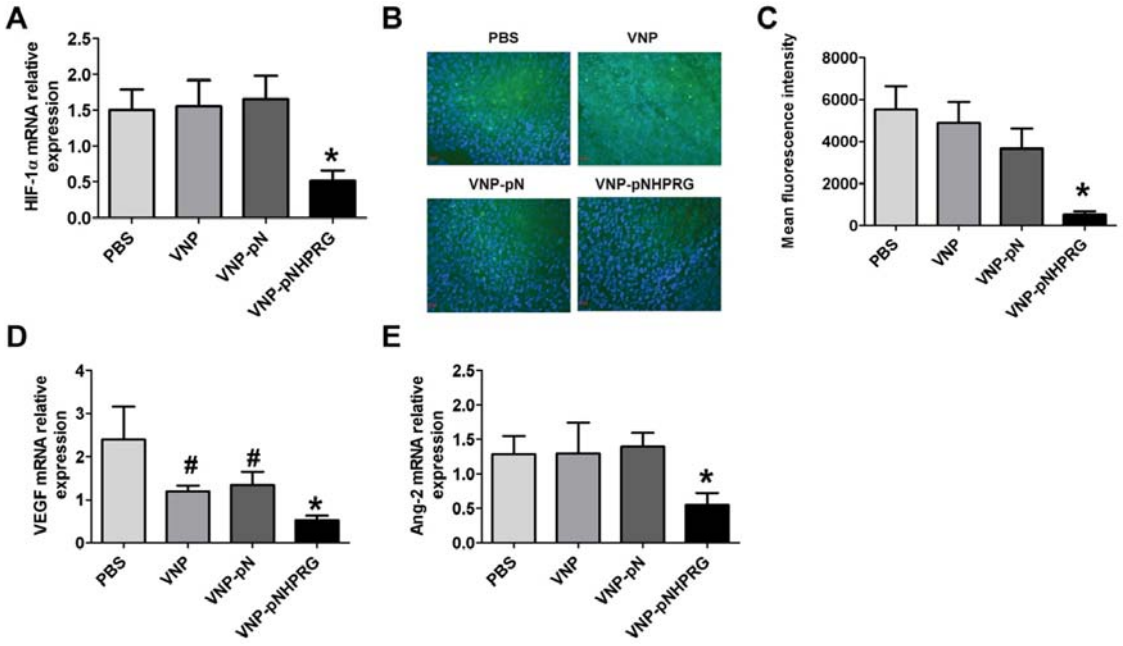

Fig. (7). VNP-pNHPRG down-regulates HIF-1α, VEGF and Ang-2 level in tumor tissues.

(**A**) HIF-1α mRNA expression levels in B16F10 tumor tissues *per* group were analyzed by real-time PCR. Bar represents the mean ± SD. n=6. *P < 0.05 for VNP-pNHPRG versus PBS, VNP and VNP-pN. (**B**) Immunofluorescence staining for HIF-1α (green) in tumor tissues of mice treated with PBS, VNP, VNP-pN and VNP-pNHPRG, shows HIF-1α expression. (**C**) Quantification showed HIF-1α expression level in tumor tissues of mice treated with PBS, VNP, VNP-pN, and VNP-pNHPRG by mean fluorescence density. *P < 0.05. VNP-pNHPRG compared with PBS, VNP and VNP-pN. Bar represents the mean ± SD of six optical fields. (**D**-**E**) VEGF mRNA and Ang-2 mRNA expression level in B16F10 tumor tissues per group were analyzed by real-time PCR. Bar represents the mean ± SD. n=6. *P < 0.05 for VNP-pNHPRG versus PBS, VNP and VNP-pN.

tumor regions, the binding capabilities of HPRG and endothelial cells increased in a lower pH microenvironment.

To assess the biological activity of HPRG *in vivo*, tumor vessel density/areas and structure were analyzed by immunofluorescence microscopy, SEM and two-photon microscopy. Compared with PBS, VNP and VNP-pN, tumor vessel density and areas significantly decreased in the B16F10 tumor model treated with VNP-pNHPRG. Compared with PBS, tumor vessel density also significantly decreased in tumor mice treated with VNP and VNP-pN. The results suggest that the reduction in tumor vessel density in tumor mice is attributed to the synergistic effect of VNP and HPRG. VNP-pNHPRG enhanced coverage percentage of pericytes in tumor vessels, but this effect was not observed in tumor vessels treated with PBS, VNP and VNP-pN. The percentage of normalized vessels in VNP-pNHPRG mice was significantly enhanced compared with that in PBS, VNP and VNP-pN mice. No statistical difference was observed among PBS, VNP and VNP-pN. The results show that VNP-pNHPRG promotes tumor vessel normalization than VNP. Given the aforementioned characteristics, VNP-pNHPRG significantly delayed tumor growth, prolonged survival time and inhibited tumor lung metastasis compared with those of PBS, VNP and VNP-pN in B16F10 tumor models.

We also explored the anticancer mechanism of VNP-pNHPRG. Aside from suppressing tumor vessel angiogenesis and promoting tumor vessel normalization, recent studies showed that the features of normalized vessel phenotype can improve tumor oxygenation and reduce hypoxic regions [46, 47]. HIF-1 is a heterodimer protein complex composed of HIF-1α and HIF-1β. Under normoxic conditions, HIF-1β is relatively stable, whereas HIF-1α binds to the von Hippel–Lindau tumor suppressor protein, which is then ubiquitylated and targeted to the proteasome for rapid degradation [48, 49]. In hypoxic conditions, HIF-1α accumulates and binds to HIF-1β, thus forming the active HIF complex that can initiate modulated expression of numerous angiogenesis genes such as VEGF and Ang-2 [50, 51]. A previous study showed that HPRG can significantly reduce hypoxic tumor regions. The reduction in hypoxic tumor regions benefits tumor oxygenation. Our study showed that VNP-pNHPRG significantly down-regulated HIF-1α protein level than PBS, VNP and VNP-pN. The down-regulation of HIF-1α protein significantly decreased VEGF and Ang-2 expression. VEGF and Ang-2 expression were found to be associated with tumor angiogenesis and tumor vessel abnormalities [52, 53]. Thus, the down-regulation of VEGF and Ang-2 expression further inhibited tumor angiogenesis and promoted tumor vessel normalization (Fig. **8**).

VNP-mediated HPRG under control of hypoxia-inducible NirB promoter can specifically express in hypoxic tumor regions. The results show that VNP-mediated HPRG therapy can inhibit tumor angiogenesis, promote tumor vessel normalization and further down-regulate the HIF-1α-VEGF/Ang-2 signal pathway by altering the hypoxic tumor microenvironment, which inhibits tumor growth and metastasis and enhances survival.

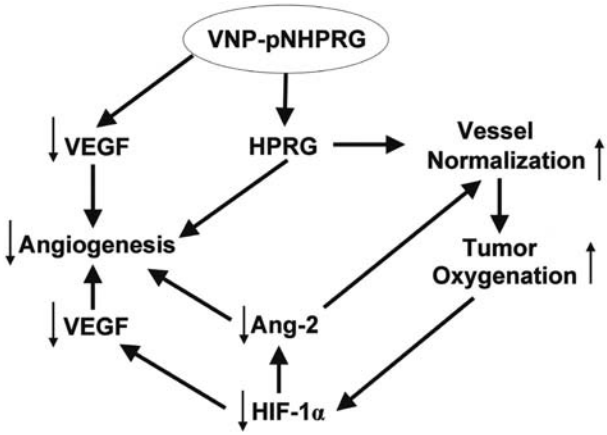

Fig. (8). The anticancer mechanism of VNP-pNHPRG.

CONFLICT OF INTEREST

The author(s) confirm that this article content has no conflicts of interest.

ACKNOWLEDGEMENTS

The authors are grateful to the grants from the Ministry of Science and Technology (2012CB967004, 2014CB 744501, 2012AA020809 and 2012ZX09401012), the Doctoral Station Science Foundation from the Chinese Ministry of Education (20130091130003), the Chinese National Natural Sciences Foundation (81121062 and 31200572), the Jiangsu Provincial Nature Science Foundation (BZ2012050, BZ2012050 and BE2013630), the Bureau of Science and Technology of Changzhou (CZ20130011, CE20135013, CZ20120004, CM20122003 and WF201207).

PATIENT CONSENT

Declared none.

SUPPLEMENTARY MATERIALS

Supplementary material is available on the publisher's web site along with the published article.

LIST OF ABBREVIATIONS

HPRG	=	Histidine-proline-rich glycoprotein
VNP	=	Attenuated *Salmonella typhimurium* strain VNP20009
NirB	=	Nitrite reductase B gene
VNPpN	=	VNP bearing the plasmid pQE30-NirB
VNPpN-HPRG	=	VNP bearing the plasmid pQE30-NirB-HPRG
VNPpN-LOL	=	VNP bearing the plasmid pQE30-Lpp-OmpA-Luciferase
VEGF	=	Vascular endothelial growth factor
Ang-2	=	Angiopoietin-2
FBS	=	Fetal Bovine Serum
LB	=	Luria-Bertani broth
H&E	=	Hematoxylin and eosin
SEM	=	Scanning electron microscope
B16F10	=	B16F10 melanoma
HUVEC	=	Human umbilical vein endothelial cell
Cfu	=	Colony forming unit
HIF-1	=	Hypoxia-inducible factor-1

REFERENCES

[1] Abe R. Angiogenesis in tumor growth and metastasis. Curr Pharm Des 2008; 14(36): 3779.

[2] Batchelor TT, Sorensen AG, di Tomaso E, *et al.* AZD2171, a pan-VEGF receptor tyrosine kinase inhibitor, normalizes tumor vasculature and alleviates edema in glioblastoma patients. Cancer Cell 2007; 11(1): 83-95.

[3] Hurwitz H, Fehrenbacher L, Novotny W, *et al.* Bevacizumab plus irinotecan, fluorouracil, and leucovorin for metastatic colorectal cancer. N Engl J Med 2004; 350(23): 2335-42.

[4] Hashizume H, Baluk P, Morikawa S, *et al.* Openings between defective endothelial cells explain tumor vessel leakiness. Am J Pathol 2000; 156(4): 1363-80.

[5] McDonald DM, Foss AJ. Endothelial cells of tumor vessels: abnormal but not absent. Cancer Metastasis Rev 2000; 19(1-2): 109-20.

[6] Abramsson A, Berlin O, Papayan H, *et al.* Analysis of mural cell recruitment to tumor vessels. Circulation 2002; 105(1): 112-7.

[7] Morikawa S, Baluk P, Kaidoh T, *et al.* Abnormalities in pericytes on blood vessels and endothelial sprouts in tumors. Am J Pathol 2002; 160(3): 985-1000.

[8] Goel S, Duda DG, Xu L, *et al.* Normalization of the vasculature for treatment of cancer and other diseases. Physiol Rev 2011; 91(3): 1071-121.

[9] Jones AL, Hulett MD, Parish CR. Histidine-rich glycoprotein: A novel adaptor protein in plasma that modulates the immune, vascular and coagulation systems. Immunol Cell Biol 2005; 83(2): 106-18.

[10] Poon IK, Patel KK, Davis DS, *et al.* Histidine-rich glycoprotein: the Swiss Army knife of mammalian plasma. Blood 2011; 117(7): 2093-101.

[11] Poon IK, Hulett MD, Parish CR. Histidine-rich glycoprotein is a novel plasma pattern recognition molecule that recruits IgG to facilitate necrotic cell clearance via FcgammaRI on phagocytes. Blood 2010; 115(12): 2473-82.

[12] Poon IK, Parish CR, Hulett MD. Histidine-rich glycoprotein functions cooperatively with cell surface heparan sulfate on phagocytes to promote necrotic cell uptake. J Leukoc Biol 2010; 88(3): 559-69.

[13] Blank M, Shoenfeld Y. Histidine-rich glycoprotein modulation of immune/autoimmune, vascular, and coagulation systems. Clin Rev Allergy Immunol 2008; 34(3): 307-12.

[14] Jones AL, Poon IK, Hulett MD, *et al.* Histidine-rich glycoprotein specifically binds to necrotic cells via its amino-terminal domain and facilitates necrotic cell phagocytosis. J Biol Chem 2005; 280(42): 35733-41.

[15] Rolny C, Mazzone M, Tugues S, *et al.* HRG inhibits tumor growth and metastasis by inducing macrophage polarization and vessel normalization through downregulation of PlGF. Cancer Cell 2011; 19(1): 31-44.

[16] Zhang L, Gao L, Zhao L, *et al.* Intratumoral delivery and suppression of prostate tumor growth by attenuated Salmonella enterica serovar typhimurium carrying plasmid-based small interfering RNAs. Cancer Res 2007; 67(12): 5859-64.

[17] Zhao M, Geller J, Ma H, *et al.* Monotherapy with a tumor-targeting mutant of Salmonella typhimurium cures orthotopic metastatic mouse models of human prostate cancer. Proc Natl Acad Sci U S A 2007; 104(24): 10170-4.

[18] Low KB, Ittensohn M, Le T, *et al.* Lipid A mutant Salmonella with suppressed virulence and TNFalpha induction retain tumor-targeting *in vivo*. Nat Biotechnol 1999; 17(1): 37-41.

[19] Clairmont C, Lee KC, Pike J, *et al.* Biodistribution and genetic stability of the novel antitumor agent VNP20009, a genetically modified strain of Salmonella typhimurium. J Infect Dis 2000; 181(6): 1996-2002.

[20] Hayashi K, Zhao M, Yamauchi K, *et al.* Cancer metastasis directly eradicated by targeted therapy with a modified Salmonella typhimurium. J Cell Biochem 2009; 106(6): 992-8.

[21] Zhao M, Yang M, Li XM, *et al.* Tumor-targeting bacterial therapy with amino acid auxotrophs of GFP-expressing Salmonella typhimurium. Proc Natl Acad Sci U S A 2005; 102(3): 755-60.

[22] Chen J, Wei D, Zhuang H, *et al.* Proteomic screening of anaerobically regulated promoters from Salmonella and its antitumor applications. Mol Cell Proteomics 2011; 10(6): M111 009399.

[23] Ganai S, Arenas RB, Forbes NS. Tumour-targeted delivery of TRAIL using Salmonella typhimurium enhances breast cancer survival in mice. Br J Cancer 2009; 101(10): 1683-91.

[24] Loeffler M, Le'Negrate G, Krajewska M, *et al.* Salmonella typhimurium engineered to produce CCL21 inhibit tumor growth. Cancer Immunol Immunother 2009; 58(5): 769-75.

[25] Toso JF, Gill VJ, Hwu P, *et al.* Phase I study of the intravenous administration of attenuated Salmonella typhimurium to patients with metastatic melanoma. J Clin Oncol 2002; 20(1): 142-52.

[26] Jia LJ, Wei DP, Sun QM, *et al.* Tumor-targeting Salmonella typhimurium improves cyclophosphamide chemotherapy at maximum tolerated dose and low-dose metronomic regimens in a murine melanoma model. Int J Cancer 2007; 121(3): 666-74.

[27] Ke N WX, Xu X, Abassi YA. The xCELLigence system for real-time and label-free monitoring of cell viability. Methods Mol Biol 2011; 740: 33-43.

[28] Keogh R. New technology for investigating trophoblast function. Placenta 2010; 31(4): 347-50.

[29] Juarez JC, Guan X, Shipulina NV, *et al.* Histidine-proline-rich glycoprotein has potent antiangiogenic activity mediated through the histidine-proline-rich domain. Cancer Res 2002; 62(18): 5344-50.

[30] Guan X, Juarez JC, Qi X, *et al.* Histidine-proline rich glycoprotein (HPRG) binds and transduces anti-angiogenic signals through cell surface tropomyosin on endothelial cells. Thromb Haemost 2004; 92(2): 403-12.

[31] Olsson AK, Larsson H, Dixelius J, *et al.* A fragment of histidine-rich glycoprotein is a potent inhibitor of tumor vascularization. Cancer Res 2004; 64(2): 599-605.

[32] Dixelius J, Olsson AK, Thulin A, *et al.* Minimal active domain and mechanism of action of the angiogenesis inhibitor histidine-rich glycoprotein. Cancer Res 2006; 66(4): 2089-97.

[33] Loeffler M, Le'Negrate G, Krajewska M, *et al.* Attenuated Salmonella engineered to produce human cytokine LIGHT inhibit tumor growth. Proc Natl Acad Sci U S A 2007; 104(31): 12879-83.

[34] Morrissey D, O'Sullivan GC, Tangney M. Tumour targeting with systemically administered bacteria. Curr Gene Ther 2010; 10(1): 3-14.

[35] Moreno M, Kramer MG, Yim L, *et al.* Salmonella as live trojan horse for vaccine development and cancer gene therapy. Curr Gene Ther 2010; 10(1): 56-76.

[36] Liu SC, Minton NP, Giaccia AJ, *et al.* Anticancer efficacy of systemically delivered anaerobic bacteria as gene therapy vectors targeting tumor hypoxia/necrosis. Gene Ther 2002; 9(4): 291-6.

[37] Dang LH, Bettegowda C, Huso DL, *et al.* Combination bacteriolytic therapy for the treatment of experimental tumors. Proc Natl Acad Sci U S A 2001; 98(26): 15155-60.

[38] Cronin M, Morrissey D, Rajendran S, *et al.* Orally administered bifidobacteria as vehicles for delivery of agents to systemic tumors. Mol Ther 2010; 18(7): 1397-407.

[39] Jiang SN, Phan TX, Nam TK, *et al.* Inhibition of tumor growth and metastasis by a combination of Escherichia coli-mediated cytolytic therapy and radiotherapy. Mol Ther 2010; 18(3): 635-42.

[40] Yu B, Yang M, Shi L, *et al.* Explicit hypoxia targeting with tumor suppression by creating an "obligate" anaerobic Salmonella Typhimurium strain. Sci Rep 2012; 2:46.

[41] Chen J, Yang B, Cheng X, *et al.* Salmonella-mediated tumor-targeting TRAIL gene therapy significantly suppresses melanoma growth in mouse model. Cancer Sci 2012; 103(2): 325-33.

[42] Jia LJ, Xu HM, Ma DY, *et al.* Enhanced therapeutic effect by combination of tumor-targeting Salmonella and endostatin in murine melanoma model. Cancer Biol Ther 2005; 4(8): 840-5.

[43] Friedlos F, Lehouritis P, Ogilvie L, *et al.* Attenuated Salmonella targets prodrug activating enzyme carboxypeptidase G2 to mouse melanoma and human breast and colon carcinomas for effective suicide gene therapy. Clin Cancer Res 2008; 14(13): 4259-66.

[44] Borza DB, Morgan WT. Histidine-proline-rich glycoprotein as a plasma pH sensor. Modulation of its interaction with glycosaminoglycans by ph and metals. J Biol Chem 1998; 273(10): 5493-9.

[45] Bensinger SJ, Christofk HR. New aspects of the Warburg effect in cancer cell biology. Semin Cell Dev Biol 2012; 23(4): 352-61.

[46] Willett CG, Boucher Y, di Tomaso E, *et al.* Direct evidence that the VEGF-specific antibody bevacizumab has antivascular effects in human rectal cancer. Nat Med 2004; 10(2): 145-7.

[47] Jain RK. Normalization of tumor vasculature: an emerging concept in antiangiogenic therapy. Science 2005; 307(5706): 58-62.

[48] Maxwell PH, Wiesener MS, Chang GW, *et al.* The tumour suppressor protein VHL targets hypoxia-inducible factors for oxygen-dependent proteolysis. Nature 1999; 399(6733): 271-5.

[49] Pugh CW, Ratcliffe PJ. Regulation of angiogenesis by hypoxia: role of the HIF system. Nat Med 2003; 9(6): 677-84.

[50] Pouyssegur J, Dayan F, Mazure NM. Hypoxia signalling in cancer and approaches to enforce tumour regression. Nature 2006; 441(7092): 437-43.

[51] Shweiki D, Itin A, Soffer D, *et al.* Vascular endothelial growth factor induced by hypoxia may mediate hypoxia-initiated angiogenesis. Nature 1992; 359(6398): 843-5.

[52] Falcon BL, Hashizume H, Koumoutsakos P, *et al.* Contrasting actions of selective inhibitors of angiopoietin-1 and angiopoietin-2 on the normalization of tumor blood vessels. Am J Pathol 2009; 175(5): 2159-70.

[53] Pore N, Jiang Z, Gupta A, *et al.* EGFR tyrosine kinase inhibitors decrease VEGF expression by both hypoxia-inducible factor (HIF)-1-independent and HIF-1-dependent mechanisms. Cancer Res 2006; 66(6): 3197-204.

Received: January 08, 2014 Revised: February 07, 2014 Accepted: February 07, 2014